Advances in Nano Research, *Vol. 9, No. 1 (2020) 59-67*
DOI: https://doi.org/10.12989/anr.2020.9.1.059

A new model for curbing filtrate loss in dynamic application of nano-treated aqueous mud systems

Emmanuel E. Okoro*[1], Bukola R. Oladejo [1], Samuel E. Sanni [2], Tamunotonjo Obomanu [3], Amarachukwu A. Ibe [4], Oyinkepreye D. Orodu [1] and Olukunle C. Olawole [5]

[1] *Petroleum Engineering Department, Covenant University, Km. 10 Idiroko Road, Ota, Nigeria*
[2] *Chemical Engineering Department, Covenant University, Km. 10 Idiroko Road, Ota, Nigeria*
[3] *Petroleum Engineering Department, Federal Polytechnic of Oil and Gas, Bonny Island, Nigeria*
[4] *Physics Department, Nigeria Maritime University, Okerenkoko, Nigeria*
[5] *Physics Department, Covenant University, Km. 10 Idiroko Road, Ota, Nigeria*

(*Received August 10, 2019, Revised June 29, 2020, Accepted July 5, 2020*)

Abstract. Filter cake formation during rotary drilling operation is an unavoidable scenario, hence there is need for constant improvement in the approaches used in monitoring the cake thickness growth in order to prevent drill-string sticking. This study proposes an improved model that predicts the growth of mud cake thickness overtime with the consideration of the addition of nanoparticles in the formulated drilling fluid system. Ferric oxide, titanium dioxide and copper oxide nanoparticles were used in varying amounts (2 g, 4 g and 6 g), and filtration data were obtained from the HPHT filtration test. The filter cakes formed were further analyzed with scanning electron microscope to obtain the morphological characteristics. The data obtained was used to validate the new filtrate loss model. This model specifically presents the concept of time variation in filter cake formation as against the previous works of constant and definite time. Regression coefficient which is a statistical measure was used to validate the new model and the predicted results were compared with the API model. The new model showed R^2 values of 99.9%, and the predictions from the proposed filtration model can be said to be more closely related to the experimental data than that predicted from the API model from the SSE and RMSE results.

Keywords: filtration model; aqueous mud system; nano particles; HPHT condition; filtrate volume; filter cake

1. Introduction

Drilling fluids perform different functions in drilling operations, and several problems encountered when drilling the wellbore is directly or indirectly related to the mud system used in the drilling operation. This is not to say that all borehole instability challenges originate from the mud system, but it is an avenue that can be used to dictate and ease instability challenges (Darley and Gray 1988, Okoro *et al*. 2018a). Aqueous and non-aqueous mud systems are the two main types of drilling fluids. Non-aqueous mud systems have several advantages in complex formations due to environmental conditions, but aqueous mud systems are commonly used during drilling operations. They usually contain water as a primary fluid, bentonite clay and many other additives, including solid and inert chemicals/ reagents, to perform many of the important functions for successful drilling (Saboori *et al*. 2012, 2019).

Bentonite is a common rheological agent for aqueous mud system because it easily dissolves, disperse and swell in a water base fluid. During drilling operation, the bentonite, polymers and other dispersed additives help in the formation of thin impermeable filter cake on the wall of the drilled hole section to avoid filtration of the mud system-based fluids (Okoro *et al*. 2018b). Filtration will occur when the mud system comes in contact with a porous filter cake and the filtrate volume is dependent on the permeability of the filter cake. High concentration of these additives may cause drilling problems such as drill-string sticking and possible formation damage; hence, it is very important to optimize the thickness of filter cake (Vipulanandan *et al*. 2014).

Reduction of filtrate volume during drilling operation can be achieved by plugging the porous filter cake formed on the wellbore wall (Okoro *et al*. 2020). The basic mechanisms of particle types from literature are macroscopic particles, microscopic particles and chemical grouting. For this study, ferric oxide, titanium dioxide and copper oxide nanoparticles were used as the plugging agent for the porous filter cakes. The aqueous mud systems were treated with these nanoparticles and during filtration test, these particles were captured near the surface and accumulated in the filter cake; since the filter cake acts like a sieve for the suspended particles. Literature has shown some models that proposed the relationship between filtration rate and the shear stress at the cake surface. Some of these models suggest that an equilibrium filter cake thickness can be controlled by an appropriate choice of suspension flow rate and filter permeability (Eltaher *et al*. 2019).

*Corresponding author, Lecturer,
E-mail: emeka.okoro@covenantuniversity.edu.ng

ISSN: 2287-237X (Print), 2287-2388 (Online)

2. Mud cake formation kinetics

The formation of filter cake is inevitable during drilling operations. Permeability damage/impairment, shale swelling and alteration of electric log resistivity curves are among the numerous reasons why the oil and gas industry are trying to determine the amount of drilling fluid filtrate that enters the borehole formation. The filter cake formed at the wellbore is subjected to varying normal and shear stresses with respect to the location in the subsurface (Vipulanandan *et al*. 2018). API model for filtration assumes that the permeability and solid fraction in the formulated filter cake is constant for the duration of drilling operation, and hence filtrate volume is believed to be directly proportional to the square-root of time with no limit to the filtrate volume. Thus, API model can be classified as a static model as shown in Eq. (1).

$$FL_f = FL_o + M * \sqrt{t} \quad (1)$$

Where FL_f is the filtrate volume, FL_o is the initial filtrate volume, t is the time and M is the model parameter.

Assumptions and gaps of API model.

- This model assumes that the cake is initially formed; moreover, this is not true because there is no cake formation at the beginning of the experiment, and in field scenario.
- It is also believed that the cake permeability remains constant, but in reality, it decreases with respect to time.
- The temperature effect is not considered, that is, it is assumed negligible.
- It is also assumed that the ratio of solids percentage in the cake to the solids percentage in the mud is also constant, but it increases with time to a limiting value when the flow stops.

Vipulanandan *et al*. (2014) proposed a filtration model that showed the relationship between filtrate volume and time. The model also accounts for changes in the permeability and thickness of filter cake with time for bentonite drilling fluids. This is an extension of the API static model. This predictive model has been proven to be effective. It has successfully predicted also the shear strain-shear rate relationship in several formulated drilling muds with varying compositions.

$$FL_f - FL_o = \frac{t}{D + E * t} \quad (2)$$

Where *D* and *E* are model parameters.

Afolabi *et al*. (2018) proposed a model that describes the impact of nanoparticles on the fluid loss of water-based mud. It considered the kinetics of the filter cake with respect to the colloidal behavior of the nanoparticles, and it has the capacity of predicting the cumulative value of the filtrate.

Limiting the extent of filtrate invasion is important (Xu *et al*. 2008), and over the past four decades, a great deal of researches and efforts have been channeled towards solving this problem; because of the emergence of new filtrate loss additives which have not been accounted for by the existing filtration-based models. The objective of this study is to characterize the nano-treated aqueous mud filter cake formed under HPHT conditions, and develop a model that will predict the short and long-term characteristics of the mud cake during drilling operation.

Table 1 Laboratory formulation of equivalent 1 barrel of WBM

Additive name	Mixing order	Mixing time (mins)	Product volume for 1 Lab. Bbl (350 mL)
Deionized water	1	0	325.13
Viscosifier	2	2	1.50
Fluid loss additive	3	1	-
Alkalinity	4	2	0.25
Salt	5	-	14.54
Others	7	2	0.50
Barite	8	5	70.0

3. Methodology

This section is in two phases; the first involves the formulation of the aqueous mud systems with three (3) nano particles (ferric oxide (Fe_2O_3), titanium dioxide (TiO_2), and copper oxide (CuO)). The second part is the development of the proposed predictive model for the formulated filter cake. Aqueous mud systems were developed using 2 g, 4 g and 6 g of the nanoparticles place the highlighted phrase in a bracket and these mud systems were subjected to HPHT filtration test. HPHT filter press half-cell was used at 200^0F and 200 psi differential pressure. The filter cakes developed during this process were analyzed and physically characterized. The data generated during this test was used to validate the proposed dynamic model developed in this study. The filter cakes formed were physically analyzed and their morphologies were determined using SEM.

3.1 Materials and formation of nano-treated aqueous drilling fluid

The materials used in the study were purchased and the details and mud compositions are tabulated in Table 1. A total of nine mud samples were formulated for this study and the samples are shown in Fig. 1. The water-based drilling fluid was prepared by dissolving 325.13 ml of deionized water with 0.25 ml caustic soda and 1.25 ml fluid loss additives for two minutes. After barite, salt, and other dispersed additives were added, the resulting suspension was mixed using a Hamilton beach mixer.

3.2 Model development

The model was developed via the following steps.

i. Formation of mud cake kinetics during filtration
ii. Colloidal behaviour of nanoparticles
iii. Derivation of the fluid loss model

(a) Ferric oxide treated mud

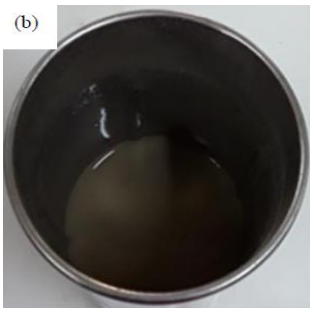

(b) Copper oxide treated mud

(c) Titanium oxide treated mud

Fig. 1 Formulated aqueous drilling fluid with three nanoparticles as filtration loss additive

Assumptions made for the new model.

i. There are changes in the permeability of the cake with time.
ii. The volume fraction of solids in the cake i.e., the ratio of the solid content in the cake to the solid content in the mud is a function of time.

The changes in the clay particles concentration in the suspension can be represented with a non-dimensional parameter, $\aleph$. The concentration of clay particles represented by CC indicates the quantity of clay particles in the suspension per time. The dimensionless parameter, clay concentration at any given time and initial concentration C_0 are related by the expression proposed by Toorman (1997).

$$\aleph = \frac{CC}{C_o} \tag{3}$$

$$(CC = C_0(\aleph) = 1) \tag{4}$$

The diffusion rate of clay particles with respect to a filter cake surface depends on the clay concentration at any given time t, and maximum concentration of clay particles in the drilling fluid $\aleph_0$ ($\aleph_0$ = 1). Therefore, the rate of diffusion thru the cake is expressed as

$$\frac{d\aleph r}{dt} = x(\aleph_0 - \aleph)^y \tag{5}$$

Where x = diffusion parameter, y = diffusion exponent.

The build-up rate of clay particles on the mud-cake is reliant on the consolidation time of particles present on the filter cake, t, and concentration of clay particles in the suspension at any time, $\aleph$. The build-up rate is stated as

$$\frac{d\aleph_b}{dt} = bt\aleph^{Cb} \tag{6}$$

Where b is the build-up constant, Cb is the build-up exponent.

A first-order kinetics is assumed for the build-up rate and diffusion rate expressions, y = Cb = 1.

$$\frac{d\aleph}{dt} = x(\aleph_o - \aleph)^y - bt\aleph^{Cb} \tag{7}$$

At equilibrium, the build-up rate equals the diffusion rate: hence $\frac{d\aleph}{dt}$ = 0.

$$x(\aleph_o - \aleph) = bt\aleph e \tag{8}$$

$$\aleph e = \frac{1}{\alpha t + 1} \tag{9}$$

Where α is the ratio of the build-up constant b to the diffusion parameter x. On the basis of cubic volumes, each δ^3, consists of a single nanoparticle. The volume of total fluid, V_T containing N nanoparticles can be expressed as

$$VT = N\delta^3 \tag{10}$$

And nanoparticles volume, V_p can be illustrated in two different but equivalent equations.

$$V_p = \varphi N\delta^3 \tag{11}$$

$$V_p = N\frac{4}{3}\pi {r_{np}}^3 \tag{12}$$

Eq. (12) assumes the nanoparticles are spherical. Equating and rearranging equations (Eqs. (11) and (12)) for the inter-particle separation distance, δ gives

$$\delta = {d_{np}}^3\sqrt{\frac{\pi}{6\varphi}} \tag{13}$$

Where, δ = inter-particle distance for rigid spheres cubically dispersed in a suspension and φ is the nanoparticle volume fraction while π (phi) is a constant.

Pouyafar and Sadough (2013), in their study introduced a dimensionless term which decreases from one to zero as shear rate increases. An explicit inter-particle distance equation was derived with respect to the presence of

nanoparticles in a cubic dispersed state. With the description of Gerogiorgis *et al*. (2017), Eq. (14) is obtained.

$$H_{np} = 4r_{np} + r_{np}\sqrt[3]{\frac{4\pi}{3\varphi}} \tag{14}$$

Where H_{np} = average distance between nanoparticles, r_{np} = nanoparticle radius, φ = fractional nanoparticles volume.

A general expression that relates the filtrate volume, V_f, behavior of a nano-treated drilling fluid, mixed with the clay particles V_{cp} and in the presence of nanoparticles V_{np} can be expressed mathematically as

$$V_f = V_{cp} + V_{np} \tag{15}$$

Darley and Gray (1988) established the API model for predicting fluid loss due to the presence of clay particles as

$${V_f}^2 = \frac{2A^2\Delta PK}{\mu}\left(\frac{V_f}{V_c}\right)t \tag{16}$$

$$\text{If,} \quad \forall = \sqrt{\frac{2A^2\Delta PK}{\mu}\left(\frac{V_f}{V_c}\right)} \tag{17}$$

$$\text{Then,} \quad V_f = \forall\sqrt{t} \tag{18}$$

According to Vipulanandan *et al*. (2014), fluid loss volume, permeability and mud cake volume are all functions of time. Thus

$$\mathrm{f}(\aleph e, K) = K\frac{1}{\alpha t + 1} \tag{19}$$

$$\mathrm{f}(\aleph e, K) = \frac{V_f}{V_{cp}} = \frac{1}{\alpha t + 1} * t \tag{20}$$

K represents the permeability of the mud cake.

Inserting Eqs. (19) and (20) into Eq. (16), gives

$$\mathrm{V}_f = \left[\frac{1 + \alpha t}{t}\right]^{-1} * \left[\sqrt{\frac{2 * \Delta P * K * A^2\left(\frac{f_{sc}}{f_{sm}}\right)}{\mu}}\right] \tag{21}$$

With the solids deposition occurring continually from the drilling fluids to the filter cake, the averaged distance will vary with change in filtration time. Therefore, as there is an increase in the inter-particle distance, the amount of solids present in the drilling fluid decreases; with respect to Gerogiorgis *et al*. (2017) method, the Van Der Waals (VDW) force of attraction between nanoparticles during filtration can be expressed as

$$F_{VDW} = \frac{r_{np}A}{12{h_{np}}^2} \tag{22}$$

Where F_{VDW} = van der Waals forces, A is identified to be the Hamaker constant, and substituting Eq. (15) into Eq. (22) gives

$$F_{VDW} = \frac{r_{np}A}{12\left[4r_{np}\left(\frac{1}{\alpha t+1}\right) + \left(1 - \frac{1}{\alpha t+1}\right) + r_{np}\sqrt[3]{\frac{4\pi}{3\varphi}}\right]^2} \tag{23}$$

Nihous (2016) mentioned that the pressure applied on the fluid column during filtration can be expressed as

$$\mathrm{P} = \rho_{fl}gh \tag{24}$$

The normal force due to hydrostatic pressure exerted on the nanoparticle is described as

$$F_{NORM} = Agh\rho_{fl} \tag{25}$$

$$F_{NORM} = g\rho_{fl}V_{np} \tag{26}$$

Where F_{NORM} = the normal force with respect to hydrostatic pressure, V_{np} = fluid loss volume with respect to the presence of nanoparticles, ρ_{fl} = fluid density, and g = acceleration due to gravity.

$$V_{np} = \frac{r_{np}A}{12g\rho_{fl}\left[4r_{np}\left(\frac{1}{\alpha t+1}\right) + \left(1 - \frac{1}{\alpha t+1}\right) + r_{np}\sqrt[3]{\frac{4\pi}{3\varphi}}\right]^2} \tag{27}$$

The proposed filtration loss model is obtained by relating the expressions of V_{np}, V_{cp} and V_f, that is

$$V_f = V_{cp} + V_{np} \tag{28}$$

From Eq. (21)

$$\mathrm{V}_{cp} = \left[\frac{1+\alpha t}{t}\right]^{-1}\left[\sqrt{\frac{2*\Delta P*K*A^2\left(\frac{f_{sc}}{f_{sm}}\right)}{\mu}}\right] \tag{29}$$

And combining all expressions together gives

$$\begin{aligned} V_f &= \left[\left[\frac{1 + \alpha t}{t}\right]^{-1}\left[\sqrt{\frac{2 * \Delta P * K * A^2\left(\frac{f_{sc}}{f_{sm}}\right)}{\mu}}\right]\right] \\ &+ \left[\frac{r_{np}A}{12g\rho_{fl}\left[4r_{np}\left(\frac{1}{\alpha t+1}\right) + \left(1 - \frac{1}{\alpha t+1}\right) + r_{np}\sqrt[3]{\frac{4\pi}{3\varphi}}\right]^2}\right] \end{aligned} \tag{30}$$

can be further expressed as

$$\begin{aligned} V_f &= \left[B\left[\sqrt{\frac{2 * \Delta P * K * A^2\left(\frac{f_{sc}}{f_{sm}}\right)}{\mu}}\right]\right] \\ &+ \left[\frac{r_{np}A}{12g\rho_{fl}\left[4r_{np}\left(\frac{1}{\alpha t+1}\right) + \left(1 - \frac{1}{\alpha t+1}\right) + r_{np}\sqrt[3]{\frac{4\pi}{3\varphi}}\right]^2}\right] \end{aligned} \tag{31}$$

Table 2 Formulated drilling fluid system properties

Mud sample	Nano particle	Weight (g)	Density (ppg)	Gel strength (lbf/100ft²)	pH	Plastic viscosity (cP)	Yield point (lbf/100ft²)
1	Fe_2O_3	2	9.7	5	11.79	15	30
2	TiO_2	2	9.7	6	11.57	14	35
3	CuO	2	9.7	5	11.47	17	28
4	Fe_2O_3	4	9.8	8	11.8	11	41
5	TiO_2	4	9.85	10	11.89	14	45
6	CuO	4	9.83	8	11.9	16	38
7	Fe_2O_3	6	9.95	9	11.91	15	41
8	TiO_2	6	9.97	11	11.9	15	49
9	CuO	6	9.84	9	11.89	16	41

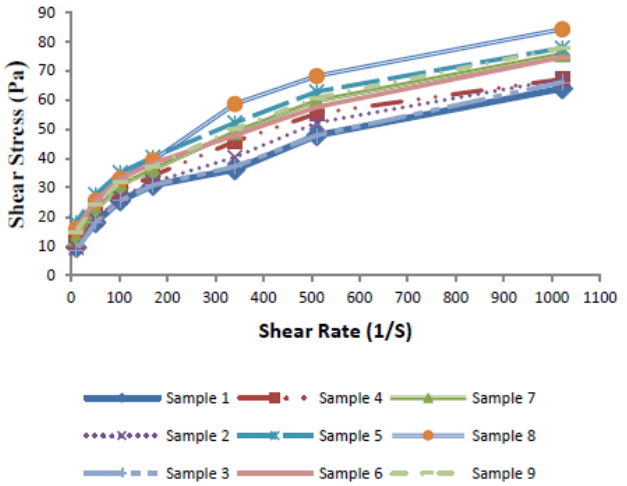

Fig. 2 Rheogram of the formulated mud systems

Where B = $\left[\frac{1+\alpha t}{t}\right]^{-1}$ represents a part of V_{cp} with respect to time.

4. Results and discussions

4.1 Formulated nano-treated aqueous mud system

Nine (9) aqueous mud system samples were formulated, samples 1, 4 and 7 contain the ferric oxide nanoparticle in varying concentrations of 2 g, 4 g and 6 g respectively; while samples 2, 5 and 8 contained titanium dioxide nanoparticles in varying concentrations. Samples 3, 6 and 9 consist of copper oxide nanoparticle in the amounts: 2 g, 4 g and 6 g respectively. Table 2 shows the drilling mud system properties, and the trend of the mud systems shows that the pH of the mud systems remained above 7; thus, it indicated that all samples are alkaline in nature as the values fall within the alkaline range. The samples containing ferric oxide NPs exhibited the highest value of pH reading. It can also be deduced that upon increasing the quantity of nanoparticles, the density increases; because the density is a ratio of mass to volume of a fluid. The specific gravity values also showed a constant increase upon the addition of

Table 3 HPHT filtration test results

Time (mins)	Formulated drilling mud system samples (mL)								
	2 g Fe_2O_3	2 g TiO_2	2 g CuO	4 g Fe_2O_3	4 g TiO_2	4 g CuO	6 g Fe_2O_3	6 g TiO_2	6 g CuO
5	15	13	12	13	13	11	9	9.4	6.8
10	10	8	7	11.2	10.9	10	8	7	6
15	12	10	10	10.2	9	9	8	7	5.2
20	15.3	14	12	11.8	10.8	8	8	7	5
25	17	16	14	10	8.4	6.8	8	7	5
30	18.8	20	16	9	8	6	8	7	5

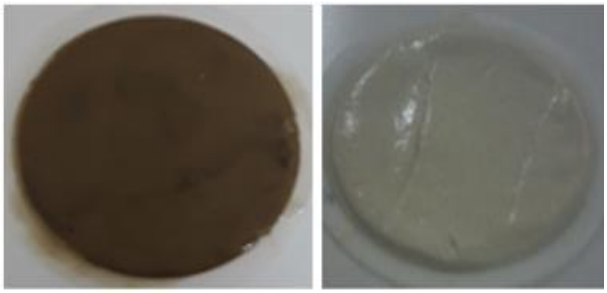

Fig. 3 Filter cake from the HPHT filtration test

the NPs in varying amount and the samples with Titanium dioxide showed the highest value.

The viscosity readings obtained from the experiments using viscometer (OFITE model 800 viscometer) were used to compute the shear stress and shear rate rheogram (Fig. 2). A rheogram is a plot that shows a non-Newtonian fluid with non-linear shear stress/shear strain relationship, which requires a finite yield stress before it begins to flow (the plot of shear stress against shear strain does not pass through the origin). For drilling fluid systems, a flow curve or rheogram is used to describe rheological properties. Fig. 2 shows that the formulated mud systems with these three nanoparticles in different amounts exhibit a non-Newtonian property, because non-Newtonian fluids do not show a linear relationship between shear stress and shear rate. This is due to the complex structure and deformation effects exhibited by the additives involved in drilling fluids.

Mud system sample 8 with 8 g of titanium dioxide had the highest shear stress and shear rate in the rheogram. The plastic viscosity values were within the standard range and the yield points for each of the mud systems were not up to three times the plastic viscosity values.

4.2 HPHT filtration analysis

The API specified test for measuring static filtration behavior of the aqueous mud systems was conducted at 380°F and 500 psi differential pressure for thirty (30) minutes. The HPHT filtrate volumes were doubled after 30 mins and tabulated in Table 3, because the cells of the equipment are half the size of the ambient filtration area. The filtrate volume from the test had a similar trend for the three nanoparticles used in this study, as the amount of the nano particle increased from 2-6 g, there was a significant

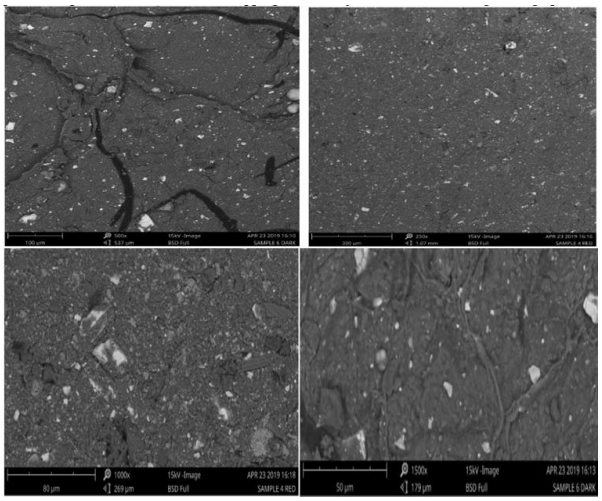

Fig. 4 SEM analysis of the filter cake morphology

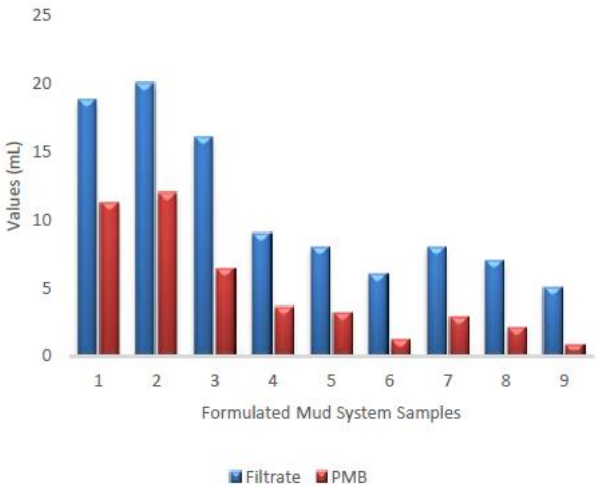

Fig. 5 HPHT filter volume and their corresponding permeability for the mud samples

Table 4 Prediction of experimental data using API and proposed models

Nanoparticles (NP, 2 g)	Experimental data (mL)	API model prediction (mL)	New model prediction (mL)
Fe_2O_3	18.8	16.9	18.6
TiO_2	20	19.2	19.9
CuO	16	15.4	16.1
NP (4 g)			
Fe_2O_3	9	8.2	8.8
TiO_2	8	7	7.8
CuO	6	5.1	5.9
NP (6 g)			
Fe_2O_3	8	6.9	7.8
TiO_2	7	6.6	6.9
CuO	5	4.1	4.9

Table 5 Regression alaysis results

Parameter	2 g cluster		4 g cluster		6 g cluster	
	API	This study	API	This study	API	This study
SSE	0.8516	0.0162	0.0179	0.0007	0.2579	0.0029
RMSE	0.9228	0.1273	0.1336	0.0267	0.5078	0.0535
R^2	0.8838	0.9978	0.9963	0.9998	0.9454	0.9994

reduction in the filtrate volume for all the mud systems.

The filter cake thicknesses formed on the filter paper during the filtration process were within 1 mm (Fig. 3).

This implies that these formulated aqueous drilling fluid samples may not pose any drill-string sticking challenges when applied in drilling oil and gas wells. The Scanning Electron Microscope (SEM) analysis in Fig. 4. shows the filter cake morphology and structural characteristics. The filter cake from the samples formed an ideal semi impermeable mud cake after the test that can prevent large volume of filtrate from slipping into the adjacent formation during drilling operation.

4.3 Estimation of filter cake permeability

The equation introduced by Von-Engelhardt and Schindewolf (2000) was adopted in this study to estimate the permeability of the filter cakes generated during the HPHT filtration test.

$$K = Q_w * Q_c * U * 1.99 * 10 \quad (33)$$

Where Q_w is the filtrate volume in ml after 30 minutes, Q_c is the filter cake thickness in cm, U is a unit constant (1), and 10 is the conversion rate to millidarcy (mD). Fig. 5. shows a comparison of the filtrate volume and the estimated filter cake permeability that gave rise to the filtrate volume. The result shows that the more porous the filter cake, the more the mud system base fluid filtrate that will pass through. Mud samples 2, 1 and 3 in this order, had the highest filtrate volume because of the high estimated permeability values; as the amount of nano particles used as filtrate loss additives were increased from 2-6 g, the filtrate volume reduced due to reduction in the filter cake permeability (PMB) by the deposition of the nano particles on the surface of the filter cake.

4.4 Validation of the new filtration model

The experimental data for the HPHT filtration tests were predicted using the API static model and the proposed filtration model, and the values generated were recorded. The recorded values were used to generate regression coefficient values (R^2) for both models and comparison was made using the experimental data as benchmark. Table 4 shows that both the API model and new model gave close values with respect to the experimental data, but the new filtration model values were more accurate compared to the API model.

The model prediction was subjected to a regression analysis, which is an explanation of causation.

Table 6 Mean absolute percentage error analysis results

Experimental data (ED)	API Model (API)	This study (NM)	ED-API	ED-NM	(ED-API)/ED	(ED-NM)/ED	l(ED-API)/ED)l	l(ED-NM)/ED)l
18.8	16.9	18.6	1.9	0.2	0.1011	0.0106	0.10106383	0.0106
20	19.2	19.9	0.8	0.1	0.0400	0.0050	0.04	0.0050
16	15.4	16.1	0.6	-0.1	0.0375	-0.00625	0.0375	0.0063
9	8.2	8.8	0.8	0.2	0.0889	0.0222	0.088888889	0.0222
8	7	7.8	1	0.2	0.1250	0.0250	0.125	0.0250
6	5.1	5.9	0.9	0.1	0.1500	0.0167	0.15	0.0167
8	6.9	7.8	1.1	0.2	0.1375	0.0250	0.1375	0.0250
7	6.6	6.9	0.4	0.1	0.0571	0.0143	0.057142857	0.0143
5	4.1	4.9	0.9	0.1	0.1800	0.0200	0.18	0.0200
SUM							0.9171	0.1451
MAPE							10.1900	1.6118

MAPE = (100%/n)*(SUM((Actual-Forecast)/Actual))

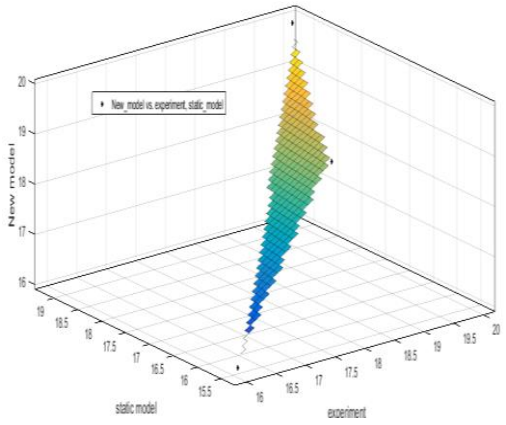

Fig. 6 Correlation coefficient for 2 g cluster

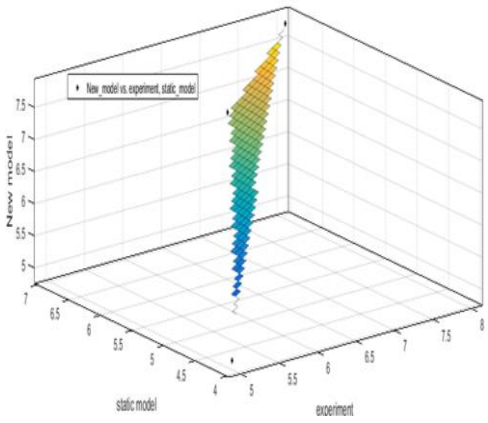

Fig. 8 Correlation coefficient for 6 g cluster

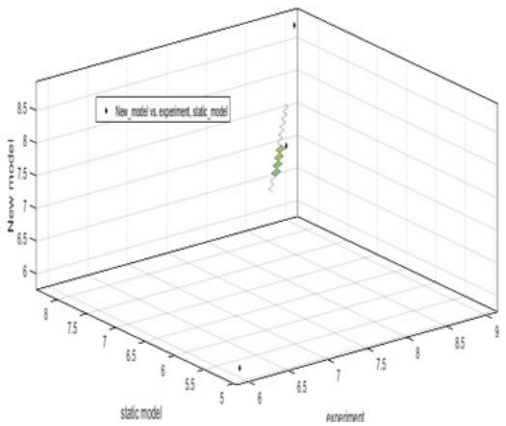

Fig. 7 Correlation coefficient for 4 g cluster

Regression analysis of the models:

Table 5 shows a summary of the regression analysis performed using the data in Table 4. The sum of squared errors (SSE) shows the sum of the squared differences between each experimental data predicted by the API and proposed filtration models and its group's mean (that is, 2 g, 4 g and 6 g clusters). If all experimental observations within a cluster are identical, the SSE would then be equal to zero. Thus, from the tabulated results, it was observed that the proposed filtration model had its SSE values closer to zero (0.0007-0.01) than the API model (0.01-0.8) for the three clusters under consideration. Root Mean Square Error (RMSE) shows how concentrated the predicted data from the models are around the line of best fit. For the API model, the RMSE values ranged from 0.1-0.9, while that of the proposed filtration model ranged from 0.02-0.1. The predictions from the proposed filtration model can be said to be more closely related to the experimental data than that predicted from the API model based on the SSE and RMSE results. R-squared (R^2) analysis is a measure of how close the predicted data fit into the regression line. It is the percentage of the response variation that is explained by a linear model. The new model gave an average R-squared value of 99.9% and this indicates that the model explains all the variability of the response data around its mean than the API model of R-squared average of 94.3%. The correlation coefficient plot for the 2 g, 4 g and 6 g clusters are present in Figs. 6, 7, and 8 respectively.

Table 6 shows the mean absolute percentage error (MAPE) for both models. MAPE is a statistical measure of how accurate a forecast system is and it is the most common measure used to forecast error. It is best for the data set for this study, because there are no extremes to the

data and no zeros. From the result interpretation, the model with smaller value of mean absolute percentage error (MAPE) is a better / appropriate model. Thus, the accuracy of the New Model (NM) is higher than that of the API, because of its lower MAPE value of 1.6118.

5. Conclusions

The prediction of filtrate loss was obtained using the newly derived filtration model. Experimental data for nine mud samples formulated with varying amount of ferric oxide, titanium dioxide and copper oxide were used for the model fitting and validation. It can be concluded from this study that:

- The proposed model gave a better explanation for the performance of the nano-treated aqueous drilling fluid.
- The new model described the quantitative contribution of nanoparticles compared to the API model.
- The nanoparticles also are good filtration loss additives. The three nanoparticles showed different visible effects upon addition to the aqueous drilling mud systems, however, copper oxide produced the least filtrate volume while titanium dioxide produced the highest filtrate volume.

Funding

This research did not receive any specific grant from funding agencies in the public, commercial, or not-for-profit sectors.

Conflict of interest

The authors have no potential conflict of interest to declare regarding the publication of this article

Acknowledgments

The authors would like to appreciate the management of Covenant University for providing an enabling environment to carry out this research, and assistance in publication.

References

Afolabi, R.O., Orodu, O.D. and Seteyeobot, I. (2018), "Predictive modelling of the impact of silica nanoparticles on fluid loss of water based drilling mud", *Appl. Clay Sci.*, **151**, 37-45. https://doi.org/10.1016/j.clay.2017.09.040

Darley, H.C. and Gray, G.R. (1988), *Composition and Properties of Drilling and Completion Fluids*, Gulf publishing company, Houston, TX, USA.

Eltaher, M.A., Almalki, T.A., Ahmed, K.I.E. and Almitani, K.H. (2019), "Characterization and behaviors of single walled carbon nanotube by equivalent-continuum mechanics approach", *Adv. Nano Res., Int. J.*, **7**(1), 39-49. https://doi.org/10.12989/anr.2019.7.1.039

Gerogiorgis, D.I., Reilly, S., Vryzas, Z., and Kelessidis, V.C. (2017), "Experimentally validated first-principles multivariate modeling for rheological study and design of complex drilling nanofluid systems", *Proceedings of SPE/IADC Drilling Conference and Exhibition*, Hague, The Netherlands, March. https://doi.org/10.2118/184692-MS

Nihous, G.C. (2016), "Notes on hydrostatic pressure", *J. Ocean Eng. Mar. Energy*, **2**, 105-109. https://doi.org/10.1007/s40722-015-0035-1

Okoro, E.E., Dosunmu, A. and Oriji, B. (2018a), "Data on cost analysis of drilling mud displacement during drilling operation", *Data Brief*, **19**, 535-541. https://doi.org/10.1016/j.dib.2018.05.075

Okoro, E.E., Lawson, K.D., Igwilo, K.C. and Ekeinde, E.B. (2018b), "One stage process removal of filtercake using micro emulsion", *Int. J. Eng. Technol*., **7**(4), 2890-2894. https://doi.org/10.14419/ijet.v7i4.13942

Okoro, E.E., Zuokumor, A.A., Okafor, I.S., Igwilo, K.C. and Orodu, K.B. (2020), "Determining the optimum concentration of multiwalled carbon nanotubes as filtrate loss additive in field-applicable mud systems", *J. Pet. Explor. Prod. Technol*., **10**, 429-438. https://doi.org/10.1007/s13202-019-0740-8

Pouyafar, V. and Sadough, S.A. (2013), "An enhanced Hershel-Bulkley model for thixotropic flow behaviour of semisolid steel alloys", *Metall. Mater. Trans B*, **44**(5), 1304-1310. https://doi.org/10.1007/s11663-013-9900-2

Saboori, R., Sabbaghi, S., Mowla, D. and Soltani, A. (2012), "Decreasing of water loss and mud cake thickness by CMC nanoparticles in mud drilling", *Int. J. NanoSci*., **8**, 171-174. https://doi.org/10.7508/IJND.2012.02.002

Saboori, R., Sabbaghi, S. and Kalantariasl, A. (2019), "Improvement of rheological, filtration and thermal conductivity of bentonite drilling fluid using copper oxide/polyacrylamide nanocomposite", *Powder Technol*., **353**, 257-266. https://doi.org/10.1016/j.powtec.2019.05.038

Toorman, E.A. (1997), "Modelling the thixotropic behaviour of dense cohesive sediment suspension", *Rheol. Acta*, **36**(1), 56-65. https://doi.org/10.1007/BF00366724

Vipulanandan, C., Raheem, A., Basirat, B., Mohammed, A. and Richardson, D. (2014), "New kinetic model to characterize the filter cake formation and fluid loss in HPHT process", *Offshore Technology Conference*, Houston, TX, USA, May. https://doi.org/10.4043/25100-MS

Vipulanandan, C., Mohammed, A. and Samuel, R.G. (2018), "Fluid loss control in smart bentonite drilling mud modified with nanoclay and quantified with vipulanandan fluid loss model", *Proceedings of Offshore Technology Conference*, TX, USA, April. https://doi.org/10.4043/28947-MS

Von Engelhardt, W. and Schindewolf, E. (2000), "The filtration of clay suspension", *Kolloid Z.*, **127**, 150-164.

Xu, T., Chen, X., LI, W. and Zhu, Q. (2008), "Equivalent cake filtration model", *Chin. J. Chem. Eng.*, **16**, 214-217. https://doi.org/10.1016/S1004-9541(08)60065-8

CC

Nomenclature

$\aleph$	Dimensionless parameter at any given time
CC	Volume fraction of clay particles at time t (dimensionless)
C_0	Initial volume fraction of clay particles (dimensionless)
$\aleph_0$	Dimensionless parameter at C_0
RPM	Revolutions per minutes
PV	Plastic Viscosity
$\aleph e$	Equilibrium parameter
α	Ratio of build-up constant to diffusion parameter (dimensionless)
φ	Nanoparticles fractional volume
N	Number of nanoparticles
r_{np}	Nanoparticle radius, nm
H_{np}	Inter-particle distance between nanoparticles, m
V_T	Total fluid volume, m^3
V_p	Nanoparticles volume, m^3
A	Hamaker constant, J
d_{np}	Nanoparticle diameter, m
V_f	Total fluid loss volume, cm^3
V_{cp}	Fluid loss volume with respect to clay particles, cm^3
V_{np}	Fluid loss Volume with respect to nanoparticles, cm^3
ΔP	Pressure applied, atm
f_{sc}	Fractional volume of solids in cake
f_{sm}	Fractional volume of solid in mud
μ	Viscosity, cp
ρ_{fl}	Fluid density, gcm^{-3}
YP	Yield Point
g	Gram
API	American Petroleum Institute
S.G	Specific Gravity
VDW	Van der Waals force
NP	Nano Particle